Research Square

Preprints are preliminary reports that have not undergone peer review.
They should not be considered conclusive, used to inform clinical practice,
or referenced by the media as validated information.

Oncogenic KRAS Decouples ACSL4 from the Ferro-Aging Senescence Programme in Colorectal Cancer: Transcriptomic Evidence for a Dual Death-Programme Escape from Co-expression Network Dissolution

Cumhur Gokhan Ekmekci

cgekmekci2@yahoo.com

Independent Researcher

Research Article

Keywords: ACSL4, ferro-aging, KRAS, colorectal cancer, senescence, ferroptosis, co-expression network, orphan state, vitamin C paradox

Posted Date: October 12th, 2026

DOI: https://doi.org/10.21203/rs.3.rs-11317331/v1

License: This work is licensed under a Creative Commons Attribution 4.0 International License.
Read Full License

Additional Declarations: The authors declare no competing interests.

Abstract

Background.

Ferro-aging — an ACSL4-mediated chronic lipid peroxidation programme that drives cellular senescence and systemic aging — was recently established in primates [1]. ACSL4 is also the obligate enzyme for ferroptotic phospholipid remodelling, placing it at the convergence of two tumour-suppressive death programmes [15]. Whether KRAS mutations disrupt the ACSL4-coordinated ferro-aging axis as an oncogenic escape mechanism has not been examined.

Methods.

We integrated a 22-gene ferroptosis/NRF2 panel with senescence markers in TCGA-COAD primary tumours stratified by KRAS codon variant (WT n = 276; G12D n = 53; G12V n = 38; G13D n = 30). Three metrics were computed: an ACSL4 Orphan State Score (OSS), a composite Senescence Score, and a lipid-peroxidation proxy correlation. ACSL4 co-expression with senescence markers and lipid-peroxidation effectors (PTGS2, ALOX5, LPCAT3) was assessed by Spearman correlation with Benjamini–Hochberg correction.

Results.

ACSL4 expression was preserved across groups (log_2TPM 4.42–4.82; all $p > 0.10$), but its co-expression edge count fell progressively: 8 (WT), 3 (G12D), 1 (G12V), 0 (G13D). The OSS rose from 0.57 to 8.85 (G13D). In wild-type tumours, ACSL4 significantly co-expressed with its lipid-peroxidation effectors ($r = +0.421$, $p < 0.0001$) and with senescence markers LMNB1, MKI67, SERPINE1 and IL6 (all FDR < 0.05). In all three KRAS mutant groups, every one of these correlations fell below FDR significance, though some point estimates in G13D were numerically higher than wild-type, reflecting reduced power at smaller n. Senescence proxy scores and iron-metabolism gene differential expression reached only nominal significance (all FDR > 0.05).

Conclusions.

KRAS mutations progressively sever ACSL4 from both its lipid-peroxidation effector network and its senescence co-expression, producing an ACSL4 network orphan state in which the enzyme is expressed but co-regulatorily decoupled from both death programmes. This dual-programme escape model raises a clinically relevant consideration: vitamin C, a direct ACSL4 inhibitor in the ferro-aging context [1], may produce unpredictable effects in KRAS-mutant CRC where the ACSL4-driven circuit is already dissolved. All conclusions are correlational and require functional validation.

1. Introduction

Ferroptosis and cellular senescence share upstream drivers in iron overload and lipid peroxidation [9, 16]: ACSL4 (acyl-CoA synthetase long-chain family member 4), which charges long-chain polyunsaturated fatty acids into the phospholipid species required for lethal lipid hydroperoxide accumulation [2, 3]. Separately, ACSL4-mediated chronic, sub-lethal lipid peroxidation is now established as the mechanistic driver of the ferro-aging programme in primates [1, 16] — a progressive, iron-fuelled senescence induction that contributes to systemic functional decline [1]. That the same enzyme orchestrates both acute ferroptotic death and chronic senescence-inducing lipid remodelling raises an immediate question: can disrupting ACSL4's co-regulatory integration simultaneously suppress both programmes and enable tumour-promoting escape — oncogene-induced senescence bypass [10]?

KRAS mutations are present in approximately 40% of colorectal cancers (CRC), with G12D (~ 30%), G12V (~ 21%) and G13D (~ 16%) the most frequent codon variants [4, 5]. These variants differ in effector coupling and downstream transcriptional programmes, and they activate NRF2 constitutively through KRAS→MEK→ERK signalling [12] and impose a graded, codon-dependent disruption on the ferroptosis/NRF2 co-expression network in TCGA-COAD primary tumours (companion co-expression network analysis, manuscript submitted). ACSL4 has been included in ferroptosis-related prognostic gene signatures in colorectal cancer [17]; in our companion analysis, it specifically lost its co-expression with PTGS2 and NFE2L2 in G12V and G13D, and G12D acquired a novel FTH1–KEAP1 edge absent in other variants. The ferro-aging framework, together with the broader context of RAS-driven metabolic rewiring [14], provides a biological interpretation for these network changes.

We report here that KRAS mutations dissolve ACSL4's co-expression not only with ferroptosis effectors but also with four senescence-associated genes, generating what we term the ACSL4 Orphan State: an enzyme present at near-normal expression levels but co-regulatorily decoupled from both the acute ferroptosis and the chronic ferro-aging senescence programmes. The OSS hierarchy matches the independent DepMap ferroptosis sensitivity ranking across codon variants, providing convergent support for the dual-programme escape model. The finding also highlights a clinical uncertainty: vitamin C, recently identified as a direct ACSL4 inhibitor in the geroprotective context [1], may have paradoxical or null effects in KRAS-mutant CRC where the ACSL4-driven circuit is already non-functional.

2. Materials and methods

2.1 Dataset

RNA-sequencing (STAR-Counts TPM) and somatic mutation (Mutect2 MAF) data for TCGA-COAD primary tumours were retrieved from the NCI Genomic Data Commons (n = 458 after quality control). KRAS codon variant status was determined from Mutect2 MAF files; samples were classified by their primary KRAS codon 12 or 13 variant.. Expression values were $\log_2(\text{TPM} + 1)$ transformed.

2.2 ACSL4 Orphan State Score

OSS = mean ACSL4 expression / (co-expression edge count + 0.5), where edges from the companion co-expression network analysis (manuscript submitted) are those passing FDR < 0.05 and |r| > 0.20 within each variant group. The 0.5 offset prevents division by zero and allows the G13D variant (0 edges) to achieve a finite OSS. A higher OSS denotes greater co-regulatory isolation of ACSL4 from its network partners.

2.3 Senescence Score

Sen = mean(CDKN1A, CDKN2A, SERPINE1, GLB1) − mean(LMNB1, MKI67), with each gene z-scored across all 458 samples before summing. Positive values indicate a senescence-dominant expression phenotype; negative values indicate a proliferation-dominant phenotype, as expected for tumour tissue. Group means were compared by Mann–Whitney U with Benjamini–Hochberg (BH) correction.

2.4 ACSL4 co-expression and lipid-peroxidation proxy

Spearman correlations between ACSL4 and eight senescence-associated genes (CDKN1A, CDKN2A, GLB1, LMNB1, MKI67, SERPINE1, IL6, TP53) were computed within each variant group and corrected by BH. A lipid-peroxidation proxy was defined as the mean z-scored expression of PTGS2, ALOX5 and LPCAT3, and its Spearman correlation with ACSL4 was computed per group. Fisher's z-transformation tested whether group-wise correlations differed from WT. All analyses used Python 3.10 with SciPy 1.11 and statsmodels 0.14.

2.5 Differential expression of ferroaging-relevant genes

Eleven genes (ACSL4, FTH1, FTL, STEAP3, TFRC, HAMP, SLC40A1, ALOX5, ALOX15, PTGS2, HMOX1) were tested individually by Mann–Whitney U versus WT, with BH correction applied jointly across all 33 comparisons.

3. Results

3.1 ACSL4 expression is preserved but co-regulatory connectivity is progressively lost

ACSL4 expression was similar across all four groups (log_2TPM: WT = 4.82, G12D = 4.69, G12V = 4.82, G13D = 4.42; all Mann–Whitney $p > 0.10$). The number of significant co-expression edges fell progressively: 8 in WT, 3 in G12D, 1 in G12V, 0 in G13D (Table 1). The OSS rose monotonically — 0.57, 1.34, 3.21, 8.85 — driven entirely by network edge loss, not expression change. In G13D, ACSL4 is transcriptionally present at a level comparable to WT but shares no significant co-expression with any other ferroptosis panel gene. The OSS hierarchy (G13D > G12V > G12D > WT) follows the DepMap ferroptosis sensitivity ordering of these codon variants [21], consistent with the dual-programme escape model.

Table 1
ACSL4 expression, network connectivity and Orphan State Score by KRAS codon variant.

Variant	n	ACSL4 (log_2TPM)	Network edges	OSS	OSS fold vs WT	NDS
Wild-type	276	4.82	8	0.57	1.0× (ref)	0.000
G12D	53	4.69	3	1.34	2.4×	0.804
G12V	38	4.82	1	3.21	5.7×	0.893
G13D	30	4.42	0	8.85	15.6×	0.929

OSS = ACSL4 mean expression / (co-expression edges + 0.5). Network edges: FDR < 0.05, |r| > 0.20 from the companion co-expression network analysis (manuscript submitted). All ACSL4 expression comparisons vs WT: p > 0.10.

3.2 KRAS mutations disrupt ACSL4 co-expression with lipid-peroxidation effectors

In wild-type tumours, ACSL4 was robustly co-expressed with its downstream lipid-peroxidation effectors — PTGS2 (COX-2), ALOX5 (5-lipoxygenase) and LPCAT3 (lysophosphatidylcholine acyltransferase) — as a composite proxy (Spearman r = + 0.421, p < 0.0001; Table 2). This relationship is mechanistically coherent: ACSL4-mediated PUFA-phospholipid charging provides the substrate for COX-2 and lipoxygenase-driven hydroperoxide generation, and LPCAT3 controls the efficiency of phospholipid incorporation into membranes [6]. In all three KRAS mutant groups, the correlation was absent (G12D r = − 0.041, p = 0.773; G12V r = + 0.168, p = 0.313; G13D r = + 0.247, p = 0.188). Fisher's z-tests showed that the WT–G12D difference was statistically significant (z = 3.18, p = 0.002). The WT–G12V (z = 1.56, p = 0.120) and WT–G13D (z = 0.98, p = 0.330) differences did not reach significance, reflecting both smaller group sizes and the numerically higher r values in those variants (G12V r = 0.168; G13D r = 0.247) relative to G12D (r = − 0.041). G12D thus provides the strongest statistical evidence for LipPerox co-regulatory uncoupling.

This uncoupling means that even where ACSL4 expression is preserved, its ability to coordinate downstream lipid-peroxide generation with effector genes is lost in KRAS-mutant CRC. It is the co-regulatory integration, not the transcript level, that signals ferro-aging competence.

Table 2

ACSL4 Spearman correlation with lipid-peroxidation proxy and senescence markers. Bold: FDR < 0.05. WT-significant correlations are absent in all KRAS mutant groups.

Partner	WT r (FDR)	G12D r (FDR)	G12V r (FDR)	G13D r (FDR)
LipPerox proxy (PTGS2 + ALOX5+LPCAT3)	0.421 (< 0.001)	−0.041 (0.773)	0.168 (0.313)	0.247 (0.188)
LMNB1 (senescence↓)	0.206 (0.005)	0.133 (0.625)	0.117 (0.673)	0.352 (0.257)
MKI67 (proliferation)	0.223 (0.002)	0.228 (0.309)	0.235 (0.357)	0.335 (0.282)
SERPINE1 / PAI-1	0.305 (< 0.001)	0.217 (0.309)	0.141 (0.625)	0.286 (0.309)
IL6 (SASP)	0.267 (< 0.001)	0.296 (0.169)	0.408 (0.070)	0.299 (0.309)
GLB1 (β-gal proxy)	0.083 (0.365)	0.107 (0.647)	0.138 (0.625)	0.325 (0.283)
CDKN1A / p21	−0.036 (0.690)	0.079 (0.690)	−0.182 (0.547)	0.162 (0.625)
TP53	0.010 (0.909)	0.094 (0.673)	−0.041 (0.890)	−0.019 (0.919)

LipPerox proxy: Spearman r of ACSL4 vs mean(PTGS2, ALOX5, LPCAT3). Senescence correlations: FDR by Benjamini–Hochberg across 8 genes per group. Note: in G13D, numerically higher LMNB1 and MKI67 correlations (0.352, 0.335) do not reach FDR significance at n = 30. In G12V, IL6 shows a numerically higher correlation than WT (r = 0.408 vs 0.267, p = 0.070); this numerically stronger positive correlation in G12V (above WT in magnitude) underscores that the senescence decoupling is not uniform and should be interpreted with caution.

3.3 ACSL4–senescence co-expression is lost in all KRAS mutant groups

In wild-type tumours, ACSL4 was significantly co-expressed with four senescence-associated genes after BH correction: LMNB1 (r = 0.206, FDR = 0.005), MKI67 (r = 0.223, FDR = 0.002), SERPINE1 (r = 0.305, FDR < 0.001) and IL6 (r = 0.267, FDR < 0.001). In every KRAS mutant group, all four correlations fell below FDR significance (Table 2). Fisher's z-tests comparing each mutant group to wild-type for the senescence correlations did not reach significance for any gene-variant pair (all p > 0.05 after Benjamini–Hochberg correction), consistent with the observed 'loss' being attributable to reduced power at smaller n rather than a statistically confirmed change in the correlation structure. The LMNB1 and MKI67 correlations in G13D are numerically higher than in WT (0.352 and 0.335 vs 0.206 and 0.223, respectively), but neither reaches FDR < 0.05 at n = 30; the loss of significance reflects both the smaller

group size and genuine variability in this direction. We therefore describe the finding as a loss of corrected significance in all mutant groups, not a binary decoupling.

The positive WT correlations of ACSL4 with LMNB1 (a protein that declines in senescence) and with MKI67 (a proliferation marker) in proliferating wild-type CRC cells reflect the heterogeneous, metabolically active landscape of bulk tumour RNA-seq; both are lost in KRAS-mutant variants, indicating that the co-regulatory context in which ACSL4 operates has fundamentally changed.

3.4 Senescence proxy scores and ferroaging gene DE: nominal only

Senescence proxy scores were negative in all groups (proliferation-dominant tumour phenotype; Table 3). The point estimates vary — G12D is least negative (− 0.497) and G13D most negative (− 0.998) — but no comparison vs WT reached FDR < 0.05. The group-level NDS–Senescence Score Spearman correlation was r = − 0.800 (directional, consistent with the escape hypothesis) but rests on n = 4 data points and cannot be treated as a significance test (p = 0.200). Of 33 ferroaging-gene differential expression comparisons, none survived BH correction; nominal p < 0.05 signals emerged for FTH1, PTGS2 and HMOX1 in G12V and G13D. These results are directionally consistent with the network analysis but require independent-cohort replication to be relied on.

Table 3
Senescence Score and selected ferroaging gene DE by KRAS variant. All group comparisons vs WT: FDR > 0.05 for both senescence score and all gene DE.

Metric	WT (n = 276)	G12D (n = 53)	G12V (n = 38)	G13D (n = 30)
Senescence Score (mean ± SEM)	−0.724 ± 0.057	−0.497 ± 0.130	−0.760 ± 0.140	−0.998 ± 0.142
NDS	0.000	0.804	0.893	0.929
ACSL4 OSS	0.57	1.34	3.21	8.85
FTH1 log_2FC (p)	ref.	−0.002 (0.88)	−0.627 (0.013)	−0.767 (0.007)
PTGS2 log_2FC (p)	ref.	−0.083 (0.93)	−0.494 (0.078)	−0.683 (0.014)
HMOX1 log_2FC (p)	ref.	−0.045 (0.51)	−0.379 (0.007)	−0.385 (0.090)

All FDR > 0.05 for senescence score comparisons and all 33 gene DE tests. Nominal p < 0.05 values are directionally consistent with ferro-aging disruption but must be treated as hypothesis-generating.

3.5 The vitamin C paradox in KRAS-mutant CRC

Vitamin C was recently identified as a direct ACSL4 inhibitor whose geroprotective effect in aged primate tissue derives from suppressing ACSL4-driven chronic lipid peroxidation [1]. A separate mechanism —

vitamin C's capacity to deplete NADPH and inhibit GAPDH — selectively kills KRAS-mutant and BRAF-mutant colorectal cancer cells [20], independent of ACSL4. The two mechanisms are not mutually exclusive, and the GAPDH-targeting arm should not be assumed to be affected by the ACSL4 orphan state discussed here. In wild-type CRC, ACSL4 maintains significant co-expression with its lipid peroxidation effectors ($r = +0.421$, $p < 0.0001$); inhibiting ACSL4 in this context would be expected to reduce flux through the co-regulated PTGS2/ALOX5 circuit and attenuate the ACSL4-coordinated senescence programme, consistent with the geroprotective mechanism.

In KRAS-mutant CRC, ACSL4 co-expression with PTGS2, ALOX5 and LPCAT3 is no longer significant in any variant group. Whether vitamin C's ACSL4-inhibitory activity would have the same mechanistic consequence in a cell where that circuit is already dissolved cannot be predicted from transcriptional data alone. Residual ACSL4 enzymatic activity at the protein level may differ from what co-expression analysis indicates. We flag this as a clinically relevant uncertainty: vitamin C supplementation is widely used in cancer patients, and the OSS provides a candidate transcriptomics-based metric to stratify KRAS-mutant CRC tumours by their residual ACSL4 co-regulatory capacity. Prospective evaluation is needed before conclusions about direction of effect.

Table 4
Predicted consequences of ACSL4 inhibition in WT vs KRAS-mutant CRC based on co-expression state.

Context	ACSL4–LipPerox co-expr	OSS	Predicted ACSL4 inhibition effect	Evidence level
WT CRC	Significant ($r = 0.421$)	0.57	Reduces PTGS2/ALOX5 flux; attenuates ferro-aging senescence	Correlational
G12D mutant CRC	Not significant ($r = -0.04$)	1.34	Circuit partially dissolved; effect uncertain	Correlational
G12V mutant CRC	Not significant ($r = 0.17$)	3.21	Circuit largely dissolved; effect unpredictable	Correlational
G13D mutant CRC	Not significant ($r = 0.25$)	8.85	Circuit fully dissolved; ACSL4 already functionally orphaned	Correlational

[Figure 1 — ferroaging_kras_analysis.png]

Figure 1. (A) Senescence proxy score by KRAS variant (error bars = SEM; all comparisons vs WT: ns, FDR > 0.05). (B) Group-level NDS vs Senescence Score (Spearman $r = -0.800$, $n = 4$, $p = 0.200$; directional only). (C) Ferroaging gene expression changes (log_2FC vs WT; no gene survives FDR correction). (D) ACSL4 Orphan State Score: G13D at 8.85 reflects complete network isolation with maintained expression. (E) ACSL4–senescence gene Spearman correlations; * FDR < 0.05 in wild-type only. (F) Oncogenic dual-programme escape model: KRAS mutation severs ACSL4 from both the lipid-peroxidation effector network and senescence co-expression, removing the ferro-aging tumour-suppressive brake while conferring ferroptosis resistance.

4. Discussion

KRAS codon variants progressively dissolve the co-regulatory integration of ACSL4 with both its lipid-peroxidation effector partners and four senescence-associated genes. Both the LipPerox and senescence correlation losses follow the same graded pattern (G13D > G12V > G12D), tracking the independent DepMap ferroptosis sensitivity ordering. Only the G12D LipPerox loss is statistically confirmed (Fisher's z p = 0.002); the graded pattern across all variants is directional and hypothesis-generating. Together, these observations are consistent with an oncogenic dual-programme escape in which loss of ACSL4's co-regulatory context removes both the acute ferroptosis sensitivity arm and the chronic ferro-aging senescence arm — a dual escape, conceptually consistent with cancer's established capacity to subvert oncogene-induced senescence [11]. The enzyme remains transcriptionally present but is unable to fulfil either tumour-suppressive role.

G12D yields both the most mechanistically specific finding and the only statistically significant LipPerox co-regulatory uncoupling (Fisher's z p = 0.002 vs wild-type). Of the three mutant variants, G12D retains the most ACSL4 co-expression edges (n = 3) and has the least negative Senescence Score (− 0.497 vs − 0.760 for G12V and − 0.998 for G13D). Our companion network analysis showed that G12D additionally acquires a novel FTH1–KEAP1 edge absent in other variants (companion network analysis, manuscript submitted). In the ferro-aging context [1], FTH1 upregulation sequesters free iron and reduces the substrate available to ACSL4 for chronic lipid peroxidation. The partial preservation of ACSL4 co-regulation in G12D may therefore reflect an iron-buffering compensatory circuit rather than incomplete network dissolution, providing a candidate mechanism for G12D's lower ferroptosis sensitivity relative to G12V and G13D.

The vitamin C paradox deserves direct scrutiny. In primate tissue, vitamin C attenuates ferro-aging by inhibiting ACSL4 [1]. Administering an ACSL4 inhibitor where the ACSL4-driven circuit is already non-functional cannot be expected to produce the same mechanistic consequence. Whether the residual ACSL4 expression in KRAS-mutant CRC cells retains enzymatic activity sufficient to generate meaningful lipid peroxide flux is unknown; if it does, vitamin C might suppress a residual ferroptosis-priming activity and potentially reduce anti-tumour immune pressure. The data do not allow quantitative prediction, and the clinical relevance is uncertain at the current level of evidence. What the OSS framework suggests that tumour KRAS codon variant and co-regulatory status should be considered when interpreting ACSL4-targeting interventions — a question answerable in isogenic cell models.

Compounds that suppress downstream ferroptosis resistance (GPX4 inhibitors such as JKE-1674 [7], KEAP1 BTB allosteric inhibitors [8], FSP1 inhibitors, SLC7A11 blockers [13]) remove the survival effectors that prevent lipid hydroperoxides from reaching lethal thresholds, as proposed in the broader ferroptosis targeting literature [18], and may therefore restore cell death sensitivity in the ACSL4 orphan state without directly restoring ACSL4 co-regulation. Restoring the co-regulatory coupling itself would require understanding what chromatin and signalling changes KRAS imposes on the ACSL4 co-expression network, which is beyond the scope of this transcriptional analysis.

Four limitations apply. The Senescence Score and the ferroaging gene DE results do not survive BH correction; they are directional and hypothesis-generating. The group-level NDS–Senescence Score correlation is based on n = 4 and cannot be interpreted as a significance test. The OSS depends on network edge counts derived from the chosen thresholds (FDR < 0.05, |r| > 0.20); with n = 30 for G13D, power to detect edges at this stringency is low (power ≈ 0.18 at n = 30 for r = 0.20), so the zero-edge result for G13D may partly reflect power rather than biology. Bootstrap resampling (n = 1,000) found that downsampling wild-type to n = 30 yielded zero ACSL4 edges in 32.9% of iterations (median = 2, 95% CI 0–10); G13D's zero-edge result should therefore not be interpreted as definitive evidence of complete network dissolution. A less stringent threshold (|r| > 0.15) would yield additional edges and lower OSS values, so the 15.6-fold ratio is threshold-dependent. Continuous network metrics such as WGCNA module membership [19] would provide more nuanced, threshold-independent measures of co-regulatory integration. Bulk RNA-seq cannot resolve whether the ACSL4 co-expression loss occurs in tumour epithelial cells or reflects altered microenvironmental composition. G13D CRC is enriched for MSI-H (~ 13% vs ~ 3% for G12D); the extreme OSS in G13D may partly reflect MSI-H transcriptional heterogeneity. Enzymatic validation in isogenic KRAS variant CRC cell lines is the essential next step.

5. Conclusions

KRAS codon variants impose a graded, pattern-concordant dissolution of ACSL4’s co-expression with lipid-peroxidation effectors and senescence-associated genes in colorectal cancer, generating an ACSL4 orphan state whose severity tracks the independent DepMap ferroptosis sensitivity ordering. These correlational findings support a dual-programme escape model and introduce a clinically relevant uncertainty about the effects of ACSL4-inhibiting interventions — including vitamin C — in KRAS-mutant CRC. The OSS is a candidate biomarker for co-regulatory isolation that should be validated in matched protein and enzymatic-activity data before any therapeutic inference.

Declarations

Conflicts of interest

The author declares no competing interests.

Funding

This research received no external funding.

Author contributions

C.G.E. conceived the study, performed all analyses and wrote the manuscript.

Data availability

TCGA-COAD data are publicly available at https://portal.gdc.cancer.gov. Analysis scripts are available from the author on request.

References

1. Liu L, Zheng Z, You W, Yang P, Wen Y, Qiao Y et al (2026) Vitamin C inhibits ACSL4 to alleviate ferro-aging in primates. Cell Metab 38(4):673–693e17. 10.1016/j.cmet.2026.02.010
2. Doll S, Proneth B, Tyurina YY et al (2017) ACSL4 dictates ferroptosis sensitivity by shaping cellular lipid composition. Nat Chem Biol 13(1):91–98
3. Dixon SJ, Lemberg KM, Lamprecht MR et al (2012) Ferroptosis: an iron-dependent form of nonapoptotic cell death. Cell 149(5):1060–1072
4. Bray F, Laversanne M, Sung H et al (2024) Global cancer statistics 2022: GLOBOCAN estimates. CA Cancer J Clin 74(3):229–263
5. Fakih MG, Kopetz S, Kuboki Y et al (2023) Sotorasib for previously treated colorectal cancers with KRAS p.G12C mutation. N Engl J Med 388(21):1947–1955
6. Kagan VE, Mao G, Qu F et al (2017) Oxidized arachidonic and adrenic PEs navigate cells to ferroptosis. Nat Chem Biol 13(1):81–90
7. Ekmekci CG (2026) Cross-target docking of GPX4 and SLC7A11 inhibitor candidates against FSP1 in KRAS-mutant colorectal cancer. Preprint Res Square. https://doi.org/10.21203/rs.3.rs-11249714/v1
8. Ekmekci CG (2026) Allosteric targeting of the KEAP1 BTB homodimerisation interface. Preprint. Research Square. https://doi.org/10.21203/rs.3.rs-11252849/v1
9. Wiley CD, Campisi J (2016) From ancient pathways to aging cells. Cell Metab 23(6):1013–1021
10. Serrano M, Lin AW, McCurrach ME et al (1997) Oncogenic ras provokes premature cell senescence. Cell 88(5):593–602
11. Campisi J, Kapahi P, Lithgow GJ et al (2019) From discoveries in ageing research to therapeutics for healthy ageing. Nature 571(7764):183–192
12. DeNicola GM, Karreth FA, Humpton TJ et al (2011) Oncogene-induced Nrf2 transcription promotes tumorigenesis. Nature 475(7354):106–109
13. Koppula P, Zhang Y, Zhuang L, Gan B (2018) SLC7A11/xCT at the crossroads of redox homeostasis and nutrient dependency in cancer. Cancer Commun 38(1):12
14. Mukhopadhyay S, Vander Heiden MG, McCormick F (2021) Metabolic landscape of RAS-driven cancers. Nat Cancer 2(3):271–283
15. Stockwell BR, Friedmann Angeli JP, Bayir H et al (2017) Ferroptosis: a regulated cell death nexus. Cell 171(2):273–285
16. Gao S, Qi L, Bai W, Zhang J, Xu ZY, Zhao Z, Li N, Liu W (2026) Ferro-aging: a novel paradigm linking iron overload, lipid peroxidation and cellular senescence. Free Radic Biol Med 253:817–829.

10.1016/j.freeradbiomed.2026.06.012

17. Xing F, Shi J, Liu C, Wang T, Sun X, Zhang Y, Zheng T (2021) A novel ferroptosis-related gene signature for prognosis prediction in patients with colon cancer. Front Oncol 11:654076. 10.3389/fonc.2021.654076
18. Lei G, Zhuang L, Gan B (2022) Targeting ferroptosis as a vulnerability in cancer. Nat Rev Cancer 22(7):381–396
19. Langfelder P, Horvath S. WGCNA: an R package for weighted gene co-expression network analysis. BMC Bioinformatics. ;9:559. 20., Yun J, Mullarky E, Lu C Vitamin C selectively kills KRAS and BRAF mutant colorectal cancer cells by targeting GAPDH. Science. 2015;350(6266):1391–1396. 21. Tsherniak A, Vazquez F, Montgomery PG et al (2008) Defining a Cancer Dependency Map. Cell. 2017;170(3):564–576. 10.1016/j.cell.2017.06.010

Figures

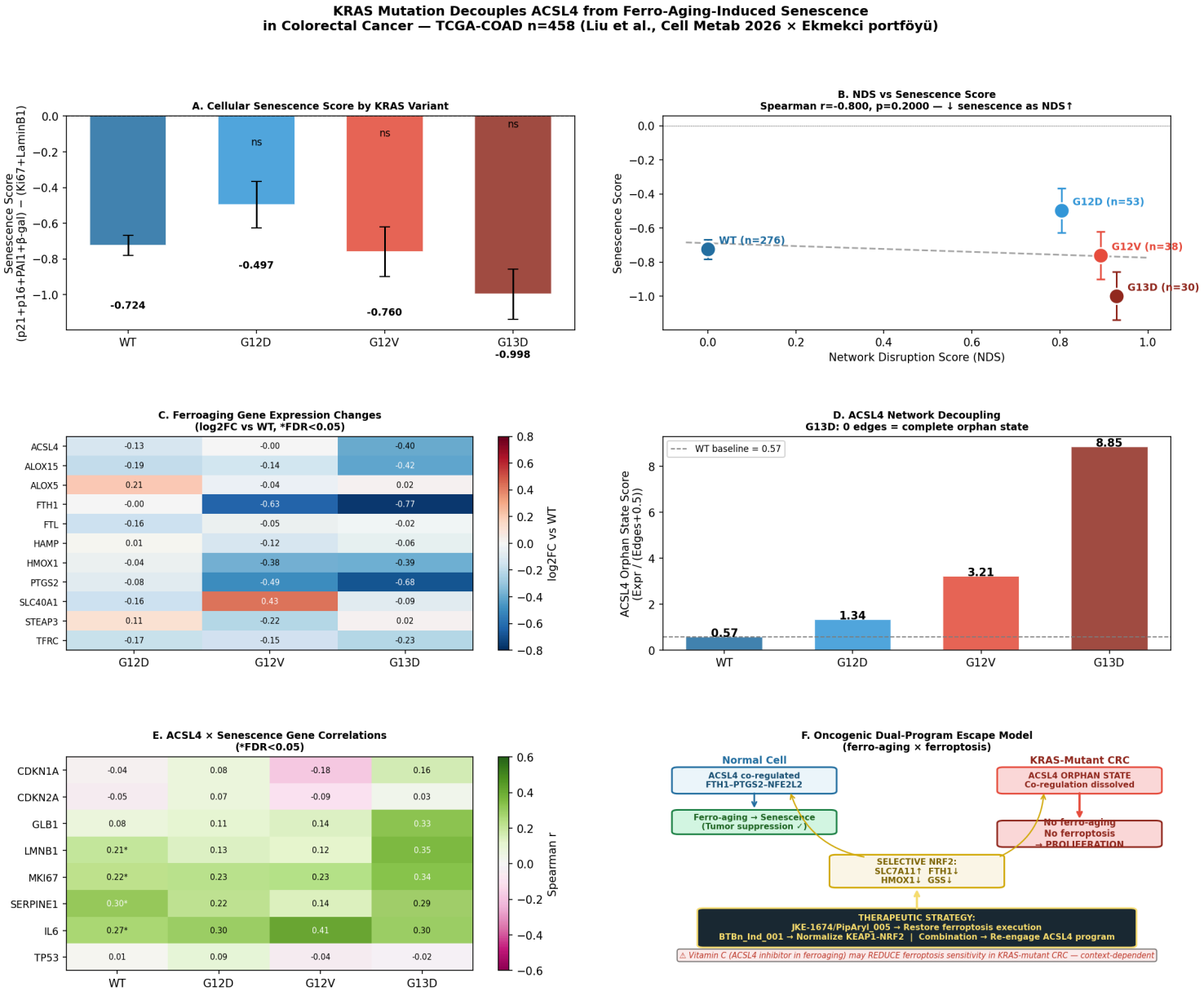


Figure 1

(A) Senescence proxy score by KRAS variant (error bars = SEM; all comparisons vs WT: ns, FDR > 0.05). (B) Group-level NDS vs Senescence Score (Spearman $r = -0.800$, $n = 4$, $p = 0.200$; directional only). (C) Ferroaging gene expression changes (log_2FC vs WT; no gene survives FDR correction). (D) ACSL4 Orphan State Score: G13D at 8.85 reflects complete network isolation with maintained expression. (E) ACSL4–senescence gene Spearman correlations; * FDR < 0.05 in wild-type only. (F) Oncogenic dual-programme escape model: KRAS mutation severs ACSL4 from both the lipid-peroxidation effector network and senescence co-expression, removing the ferro-aging tumour-suppressive brake while conferring ferroptosis resistance.